The Galactic Center: Feeding and Feedback in a Normal Galactic Nucleus
Proceedings IAU Symposium No. 303, 2013
L. O. Sjouwerman, C. C. Lang & J. Ott

doi:10.1017/S1743921314000398

A radio survey of Galactic center clouds

E. A. C. Mills[1], C. C. Lang[2], M. R. Morris[3], J. Ott[1], N. Butterfield[2], D. Ludovici[2], S. Schmitz[2] and A. Schmiedeke[4]

[1]National Radio Astronomy Observatory, USA (email: bmills@aoc.nrao.edu) [2]Dept. of Physics & Astronomy, University of Iowa, USA [3]Dept. of Physics & Astronomy, University of California-Los Angeles, USA [4]I. Physikalisches Institut, Universität zu Köln, Germany

Abstract. We present a radio survey of molecules in a sample of Galactic center molecular clouds, including M0.25 + 0.01, the clouds near Sgr A, and Sgr B2. The molecules detected are primarily NH_3 and HC_3N; in Sgr B2-N we also detect non-metastable NH_3, vibrationally-excited HC_3N, torsionally-excited CH_3OH, and numerous isotopologues of these species. 36 GHz Class I CH_3OH masers are ubiquitous in these fields, and in several cases are associated with new NH_3 (3,3) maser candidates. We also find that NH_3 and HC_3N are depleted or absent toward several of the highest dust column density peaks identified in submillimeter observations, which are associated with water masers and are thus likely in the early stages of star formation.

Keywords. Galaxy: center — molecular data — radio lines: ISM — techniques: interferometric

---

The central 300 parsecs of the Galaxy contain one of the largest reservoirs of molecular gas in the Galaxy. Thus far, however, the large-scale distribution and kinematics of this molecular gas have only been probed at arcminute ($\sim$ 2-3 pc) resolutions (e.g., Bally *et al.* 1987, Jones *et al.* 2013). This survey is a first step toward a uniform study of Galactic center gas on sub-parsec scales. Ultimately, these survey data will probe the temperatures, densities, and kinematics of a sample of clouds at 2-3″ ($\sim$0.1 pc) resolution.

1. Observations and data calibration

Observations were made using the new WIDAR correlator in the hybrid DnC array of the Karl G. Jansky Very Large Array (VLA). Ka-band data (27-36 GHz) were observed on 2012 January 7 and 13, and K-band data (24-25 GHz) on 2012 January 8 and 14. The data consist of 18 pointings toward 6 clouds (Sgr B2 M&N, M0.25 + 0.01, M-0.11-0.08, M−0.02−0.07, the CND, and M−0.13−0.08).

The survey was designed to cover a large number of NH_3 transitions, which trace gas with densities $\gtrsim 10^3$ cm^{-3}, and can be used to measure kinetic temperature. Eight transitions of NH_3 with energies from 20 to 840 K above the ground state are observed, which are collectively sensitive to a wide range of gas temperatures. In addition, the observations cover multiple transitions of HC_3N and CH_3OH.

The observations in each band (K and Ka) are divided into two separate, continuous subbands 0.86 GHz wide, each comprised of 7 spectral windows. The typical spectral resolution is 250 kHz ($\sim$ 3 km s^{-1}), however for three spectral windows, covering (1) the NH_3 (1,1) and (2,2) lines and their hyperfine structure, (2) the 36.1 GHz CH_3OH maser line, and (3) the CH_3CN (2_k-1_k) transitions, the resolution is doubled to better resolve the line structure.

The phase calibrator (J1744−3116) was observed approximately every 15 minutes. The bandpass calibrator was J1733−1304. The data were flux calibrated using 3C286, observed at elevations comparable to the Galactic center sources ($\sim 15^\circ - 30^\circ$).

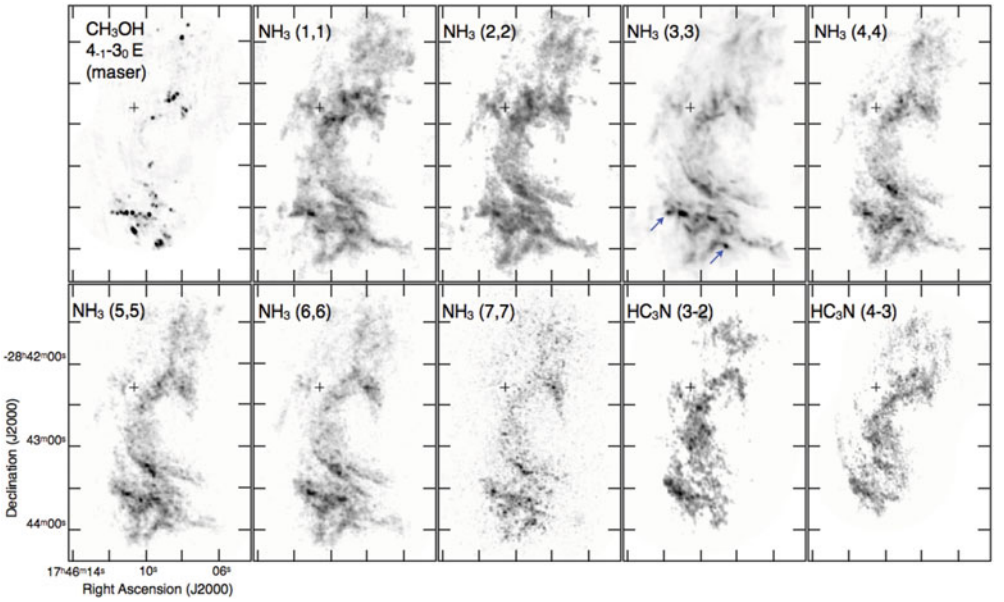

Figure 1. Peak intensity maps of molecular lines in M0.25 + 0.01, including 36 GHz methanol masers, 7 transitions of NH_3, and two transitions of HC_3N. The cross indicates the location of an H_2O maser (Lis *et al.* 1994) coinciding with a dust continuum peak (Kauffmann *et al.* 2013). Examples of candidate NH_3 (3,3) masers are indicated with arrows.

After calibration with the *CASA* reduction package, the data were imaged using the CLEAN algorithm in *CASA* and a CLEAN cycle of several thousand iterations, resulting in noise in the final images which was typically ∼1 mJy beam^{-1} channel^{-1} for the spectral line images. The full width at half maximum (FWHM) of the synthesized clean beam ranged from $2\farcs3 \times 2\farcs5$ at 25 GHz to $1\farcs9 \times 2\farcs2$ at 27 GHz and $1\farcs5 \times 1\farcs7$ at 36 GHz.

2. Results

We present preliminary images of M0.25 + 0.01, clouds near Sgr A, and Sgr B2.

M0.25 + 0.01: This cloud is one of the most massive in the central molecular zone (CMZ) (M∼ $1 - 2 \times 10^5$ $M_\odot$; Lis *et al.* 1994, Longmore *et al.* 2012). However, unlike other massive CMZ clouds, there is no evidence in this cloud for ongoing star formation apart from a single water maser (Lis *et al.* 1994, Longmore *et al.* 2012, Kauffmann *et al.* 2013).

Mapping this cloud, we find the morphology of the NH_3 transitions is almost identical (apart from a few candidate masers in the (3,3) lines; Figure 1): there is no sign of temperature gradients. The (1,1) and (2,2) transitions are both very optically-thick, (τ up to 4-7), as measured from the ratio of their hyperfine satellites. From the optically-thin (4,4), (5,5), and (7,7) lines, we measure a median temperature of ∼100 K.

The distribution of HC_3N is similar to NH_3, but is stronger toward the center of the cloud, and may trace denser gas. We also detect numerous 36.1 GHz CH_3OH point sources, the distribution of which closely follows the morphology of the NH_3 gas (Figure 1). The majority of the CH_3OH sources are relatively weak, with intensities of 0.5 - 1 Jy beam^{-1}. However, more than 80% can be identified as masers, having brightness temperatures greater than the hottest gas identified in this cloud (400 K; Mills & Morris 2013). Dozens of such candidate masers are found in every cloud surveyed. As

https://doi.org/10.1017/S1743921314000398 Published online by Cambridge University Press

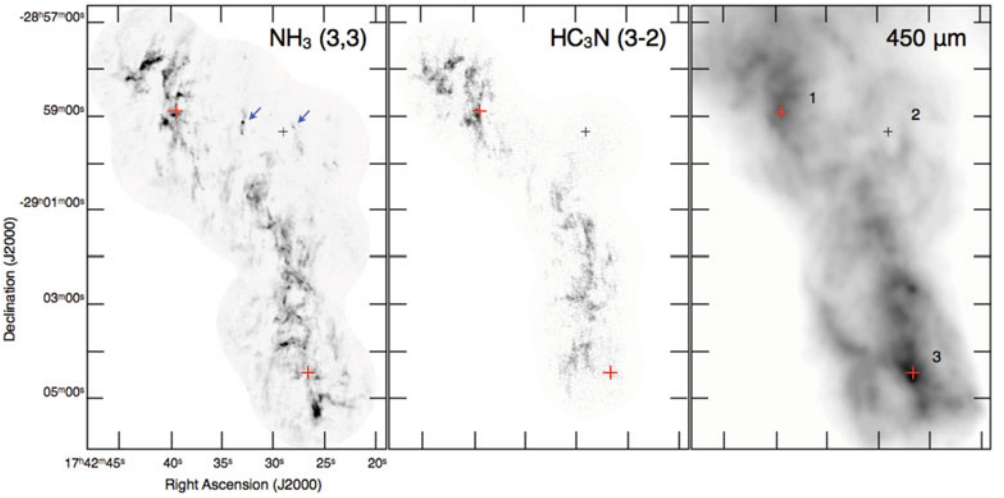

Figure 2. Peak intensity maps of NH_3 (3,3) (**left**) and HC_3N 3-2 (**center**) in Sgr A, compared to 450 micron dust continuum (**Right**; Pierce-Price *et al.* 2000). Crosses indicate dust continuum peaks in M−0.02−0.07 (1), M−0.13−0.08 (3), and the location of the supermassive black hole Sgr A* (2). Examples of candidate NH_3 (3,3) masers are indicated with arrows. [A color version is available online.]

these are Class I masers, they are indicative of shocks, but in the turbulent environment of the Galactic center, they likely do not indicate star formation.

Sgr A: There are three main clouds near Sgr A: M−0.02−0.07, M−0.13−0.08, and the circumnuclear disk (CND), which surrounds the supermassive black hole, Sgr A*. In projection, these clouds lie within the central 10 pc of the Galaxy, and are believed to be physically close as well, based upon their interactions with each other and with the gravitational potential of Sgr A* (Coil & Ho 2000, Herrnstein & Ho 2005).

The strongest sources of NH_3 emission are M−0.02−0.07, and a clump at the southern tip of M−0.13−0.08 (Figure 2). However, this clump is entirely absent in HC_3N. As in M0.25 + 0.01, there is also no NH_3 or HC_3N detected toward the strongest dust continuum peak in M−0.13−0.08 and its associated H_2O masers (Guesten & Downes 1983; Sjouwerman *et al.* 2002).

HC_3N is not detected toward the CND, which is either an indication that gas in this region is less dense, or that HC_3N is under-abundant or destroyed in this environment (Martín *et al.* 2012). NH_3 emission from the CND is weak in comparison to emission from M−0.02−0.07 and M−0.13−0.08, although several strong, compact sources of NH_3 (3,3) emission (likely masers) are found here, coincident with observed 36 and 44 GHz CH_3OH masers (Sjouwerman *et al.* 2010, Yusef-Zadeh *et al.* 2008).

Sgr B2: This is the most massive Galactic center cloud, and hosts extremely active star formation traced by dozens of ultracompact HII regions (e.g., De Pree *et al.* 1998).

The structure of the cloud, as seen in NH_3 (3,3), is a wide filament oriented in the southeast/northwest direction (Figure 3). NH_3 (3,3) emission is detected from the 'N' and 'M' sub-millimeter cores, as well as likely (3,3) masers in the south (Martín-Pintado *et al.* 1999). Emission from most other molecules is confined to N, although all three sub-millimeter cores (N,M,S) are detected in J_2-J_1 E-type CH_3OH transitions. In the primary hot core in N (SMA-1, v∼63 km s^{-1}), emission from these lines of CH_3OH and its ^{13}C isotopologue, as well as from a torsionally-excited line of A^+-type CH_3OH (12_2- 11_1, v_T=1) traces a ringlike structure of diameter 5″ (Figure 3), first mapped in CH_3CH_2CN

https://doi.org/10.1017/S1743921314000398 Published online by Cambridge University Press

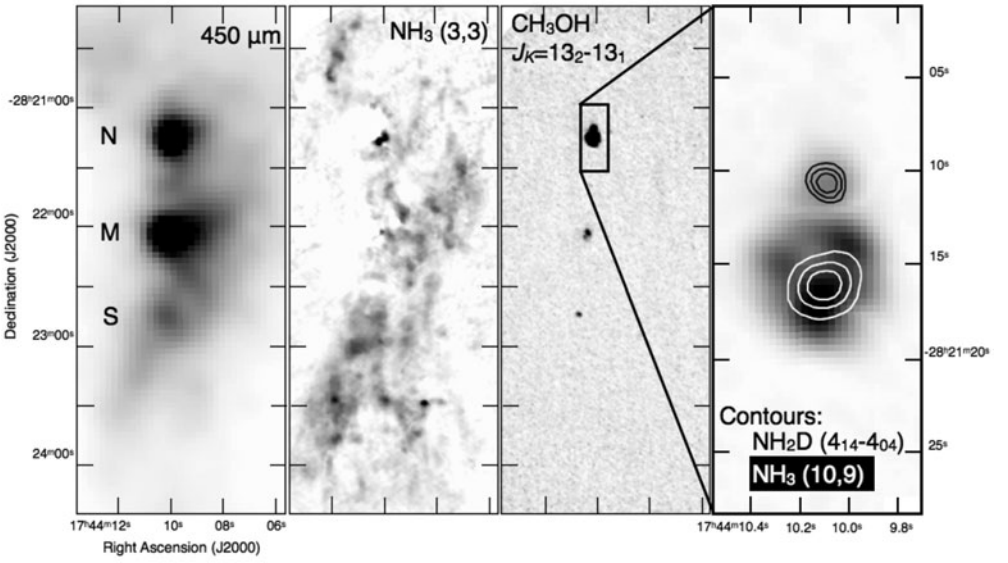

Figure 3. Peak intensity maps of NH_3 (3,3) (**center**) and CH_3OH 13_2-13_1 (**Rightmost two** panels) in Sgr B2, compared to 450 micron dust continuum (**Left**; Pierce-Price *et al.* 2000). The **far-right** panel shows a zoom of Sgr B2-N and the two hot cores: SMA-1 (white contours) the most chemically-rich source in this survey and the location of the strongest non-metastable NH_3 emission, and SMA-2 (black contours), where we detect NH_2D.

(Hollis *et al.* 2003). A second hot core in N (SMA-2, $v \sim$75 km s^{-1}, 5″ to the north; Liu & Snyder 1999, Qin *et al.* 2011) is also seen in the J_2-J_1 lines of CH_3OH and $^{13}CH_3OH$.

Metastable NH_3 emission in SMA-1, as previously detected by Vogel *et al.* (1987), is extremely optically thick: hyperfine satellites are clearly detected in all lines, including (9,9). Emission from the NH_3 satellite lines (which are more optically thin than the main lines) as well as the optically-thin isotopologue $^{15}NH_3$, peaks on the southern edge of this ring, and is roughly co-spatial with emission from vibrationally-excited transitions of HC_3N and non-metastable NH_3. However, the 4_{14}-4_{04} transition of singly-deuterated ammonia (NH_2D) is not detected toward SMA-1, and is only seen toward SMA-2, suggesting the deuterated fraction of this core may be higher than previously estimated for 'N' as a whole (Peng *et al.* 1993).

References

Bally, J., Stark, A., Wilson, T. L., & Henkel, C. 1987, *ApJS* 65, 13
Coil, A. L. & Ho, P. T. P. 2000, *ApJ* 533, 245
De Pree, C. G., Goss, W. M., & Gaume, R. A. 1998, *ApJ* 500, 847
Güsten, R. & Downes, D. 1983, *A&A* 117, 343
Herrnstein, R. M. & Ho, P. T. P. 2005, *ApJ* 620, 287
Hollis, J. M., Pedelty, J. A., Boboltz, D. A., Liu, S.-Y., Snyder, L. E., *et al.* 2005, *ApJ* 596, L235
Jones, P. A., Burton, M. G., Cunningham, M. R., Tothill, N., & Walsh, A. 2005, *MNRAS* 433, 221
Kauffmann, J., Pillai, T., & Zhang, Q. 2013, *ApJ* 765, L35
Lis, D. C., Menten, K. M., Serabyn, E., & Zylka, R. 1994, *ApJ* 423, L39
Liu, S.-Y. & Snyder, L. E. 1999, *ApJ* 523, 683
Longmore, S. N., Rathborne, J., Bastian, N., Alves, J., Ascenso, J., *et al.* 2005, *ApJ* 746, 117
Martín, S., Martín-Pintado, J., Montero-Castaño, M., Ho, P. T. P., *et al.* 2012, *A&A* 539, 21

https://doi.org/10.1017/S1743921314000398 Published online by Cambridge University Press

Martín-Pintado, J., Gaume, R. A., Rodríguez-Fernández, N., *et al.* 1999, *ApJ* 519, 667
Mills, E. A. C. & Morris, M. R. 2013, *ApJ* 772, 105
Peng, Y., Vogel, S. N., & Carlstrom, J. E. 1993, *ApJ* 418, 255
Pierce-Price, D., Richer, J. S., Greaves, J. S., Holland, W. S., *et al.* 2000, *ApJ* 545, L121
Qin, S. L., Schilke, P., Rolffs, R., Comito, C., Lis, D. C., & Zhang, Q. 2011, *A&A* 530, L9
Sjouwerman, L. O., Lindqvist, M., van Langevelde, H. J., & Diamond, P. J. 2002, *A&A* 391, 967
Sjouwerman, L. O., Pihlström, Y. M., & Fish, V. L. 2010, *ApJ* 710, L111
Vogel, S. N., Genzel, R., & Palmer, P. 1987, *ApJ* 316, 243
Yusef-Zadeh, F., Braatz, J., Wardle, M., & Roberts, D. 2008, *ApJ* 683, L147

https://doi.org/10.1017/S1743921314000398 Published online by Cambridge University Press